

First-in-Human Phase I Study of Fisogatinib (BLU-554) Validates Aberrant FGF19 Signaling as a Driver Event in Hepatocellular Carcinoma



Richard D. Kim¹, Debashis Sarker², Tim Meyer³, Thomas Yau⁴, Teresa Macarulla⁵, Joong-Won Park⁶, Su Pin Choo⁷, Antoine Hollebecque⁸, Max W. Sung⁹, Ho-Yeong Lim¹⁰, Vincenzo Mazzaferro¹¹, Joerg Trojan¹², Andrew X. Zhu¹³, Jung-Hwan Yoon¹⁴, Sunil Sharma¹⁵, Zhong-Zhe Lin¹⁶, Stephen L. Chan¹⁷, Sandrine Faivre¹⁸, Lynn G. Feun¹⁹, Chia-Jui Yen²⁰, Jean-Francois Dufour²¹, Daniel H. Palmer²², Josep M. Llovet^{9,23}, Melissa Manogian²⁴, Meera Tugnait²⁵, Nicolas Stransky²⁵, Margit Hagel²⁵, Nancy E. Kohl²⁵, Christoph Lengauer²⁵, Cori Ann Sherwin²⁵, Oleg Schmidt-Kittler²⁵, Klaus P. Hoeflich²⁵, Hongliang Shi²⁵, Beni B. Wolf²⁵, and Yoon-Koo Kang²⁶

ABSTRACT

Outcomes for patients with advanced hepatocellular carcinoma (HCC) remain poor despite recent progress in drug development. Emerging data implicate FGF19 as a potential HCC driver, suggesting its receptor, FGFR4, as a novel therapeutic target. We evaluated fisogatinib (BLU-554), a highly potent and selective oral FGFR4 inhibitor, in a phase I dose-escalation/dose-expansion study in advanced HCC using FGF19 expression measured by IHC as a biomarker for pathway activation. For dose escalation, 25 patients received 140 to 900 mg fisogatinib once daily; the maximum tolerated dose (600 mg once daily) was expanded in 81 patients. Fisogatinib was well tolerated; most adverse events were manageable, grade 1/2 gastrointestinal events, primarily diarrhea, nausea, and vomiting. Across doses, the overall response rate was 17% in FGF19-positive patients [median duration of response: 5.3 months (95% CI, 3.7–not reached)] and 0% in FGF19-negative patients. These results validate FGFR4 as a targetable driver in FGF19-positive advanced HCC.

SIGNIFICANCE: Fisogatinib elicited clinical responses in patients with tumor FGF19 overexpression in advanced HCC. These results validate the oncogenic driver role of the FGFR4 pathway in HCC and the use of FGF19 as a biomarker for patient selection.

See related commentary by Subbiah and Pal, p. 1646.

¹H. Lee Moffitt Cancer Center and Research Institute, Tampa, Florida. ²King's College London, London, United Kingdom. ³University College London, London, United Kingdom. ⁴Queen Mary Hospital, Hong Kong, China. ⁵Vall d'Hebron University Hospital and Vall d'Hebrón Institute of Oncology (VHIO), Barcelona, Spain. ⁶National Cancer Center Korea, Goyang, South Korea. ⁷National Cancer Centre Singapore, Singapore. ⁸Institute Gustav Roussy, Villejuif, France. ⁹Mount Sinai Liver Cancer Program, Tisch Cancer Institute, Icahn School of Medicine at Mount Sinai, New York, New York. ¹⁰Samsung Medical Center, Sungkyunkwan University, Seoul, Korea. ¹¹University of Milan, Department of Oncology and Istituto Nazionale Tumori, IRCCS Foundation, Department of Surgery, HPB Surgery and Liver Transplantation, Milan, Italy. ¹²Universitätsklinikum Frankfurt, Frankfurt, Germany. ¹³Massachusetts General Hospital, Harvard Medical School, Boston, Massachusetts. ¹⁴Seoul National University Hospital, Seoul, South Korea. ¹⁵Huntsman Cancer Institute, Salt Lake City, Utah. ¹⁶National Taiwan University Hospital, Taipei, Taiwan. ¹⁷State Key Laboratory of Translational Oncology, The Chinese University of Hong Kong, Hong Kong, China. ¹⁸Hôpitaux Universitaires Paris Nord Val de Seine, Paris, France. ¹⁹University of Miami, Miami, Florida. ²⁰National Cheng Kung University Hospital,

College of Medicine, National Cheng Kung University, Tainan, Taiwan. ²¹University Clinic for Visceral Surgery and Medicine, Inselspital Bern, Bern, Switzerland. ²²Liverpool Experimental Cancer Medicine Centre, Liverpool, United Kingdom. ²³Translational Research in Hepatic Oncology Group, Liver Unit, IDIBAPS, Hospital Clinic, University of Barcelona, Barcelona, Catalonia, Spain. ²⁴Roche Tissue Diagnostics, Tucson, Arizona. ²⁵Blueprint Medicines Corporation, Cambridge, Massachusetts. ²⁶Asan Medical Center, University of Ulsan College of Medicine, Seoul, South Korea.

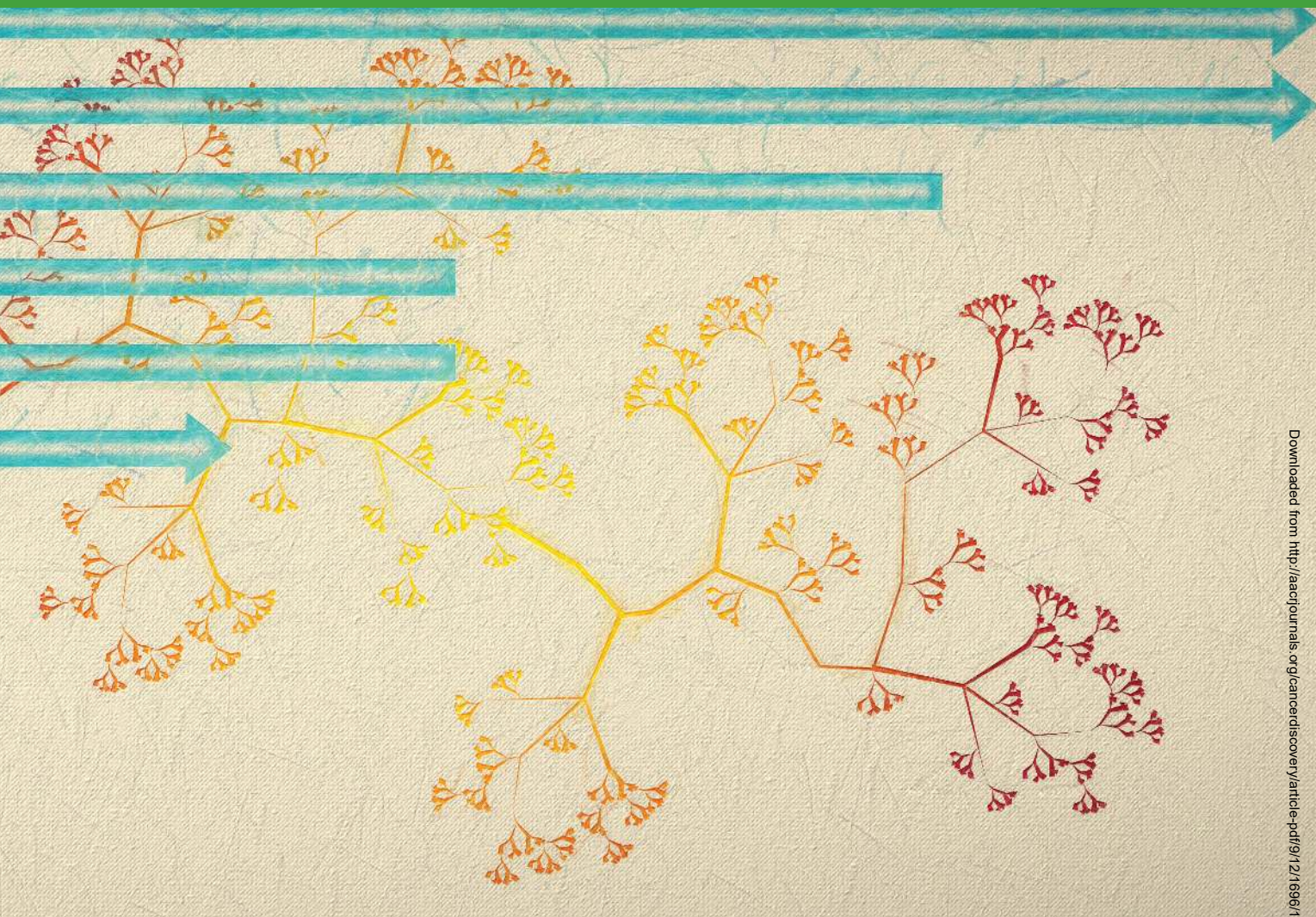
Note: Supplementary data for this article are available at Cancer Discovery Online (<http://cancerdiscovery.aacrjournals.org/>).

Corresponding Author: Yoon-Koo Kang, Asan Medical Center, 88, Olympic-ro 43-gil, Songpa-gu, Seoul 05505, South Korea. Phone: 82-2-3010-3230; Fax: 82-2-3010-8772; E-mail: ykkang@amc.seoul.kr

Cancer Discov 2019;9:1696–707

doi: 10.1158/2159-8290.CD-19-0555

©2019 American Association for Cancer Research.



Downloaded from <http://aacrjournals.org/cancerdiscovery/article-pdf/9/12/1696/1840349/1696.pdf> by guest on 27 August 2022

INTRODUCTION

Hepatocellular carcinoma (HCC), the most common primary liver cancer, is a leading cause of cancer morbidity and mortality throughout the world, with 841,000 new cases and more than 781,000 deaths worldwide in 2018 (1, 2); despite recent advances in drug development, the outcome for patients with advanced HCC remains poor. Currently approved treatments for HCC in the first-line setting include the multikinase inhibitors sorafenib and lenvatinib. Second-line treatments include the multikinase inhibitors cabozantinib and regorafenib, the anti-VEGF antibody ramucirumab, and the anti-PD-1 antibodies nivolumab and pembrolizumab (3). Although anti-PD-1 antibodies are associated with encouraging response durations, most patients do not achieve an objective response. With these available treatments, median progression-free survival (PFS) and overall survival remain in the ranges of 3 to 7 months and 9 to 13 months, respectively (4–10). Thus, there is a critical unmet need for improved novel treatments for HCC.

Emerging data implicate FGF19 as a potential HCC driver and suggest its receptor, the tyrosine kinase FGFR4, as a novel therapeutic target. FGF19 normally functions as an

ileum-derived postprandial hormone that regulates bile-acid synthesis and hepatocyte proliferation via signaling through FGFR4 and its coreceptor klotho- β (KLB; ref. 11). However, several studies have demonstrated aberrant FGF19 expression in a subset of HCC, potentially implicating FGF19 as a driver of hepatocarcinogenesis (12, 13). FGF19 overexpression in patients with HCC occurs via genomic amplification of the *FGF19/CCND1* locus on chromosome 11q13.3 (~6% of cases; refs.13–15) or via epigenetic mechanisms that upregulate *FGF19* mRNA/protein (~23% of cases; ref. 16). In either case, aberrant expression of FGF19 may create an autocrine-paracrine signaling loop in which the ligand binds to FGFR4 and KLB and initiates downstream signaling that promotes HCC proliferation and survival. Preclinical data support this idea by showing that ectopic FGF19 expression *in vitro* promotes HCC proliferation, and transgenic FGF19 expression in mice causes HCC (17, 18). Targeting FGFR4 with antibodies (19) or small-molecule inhibitors (20) attenuates tumor growth in HCC preclinical models, demonstrating the therapeutic potential of this pathway. In a recent study, *FGF19* amplification was independently associated with shorter survival and a higher

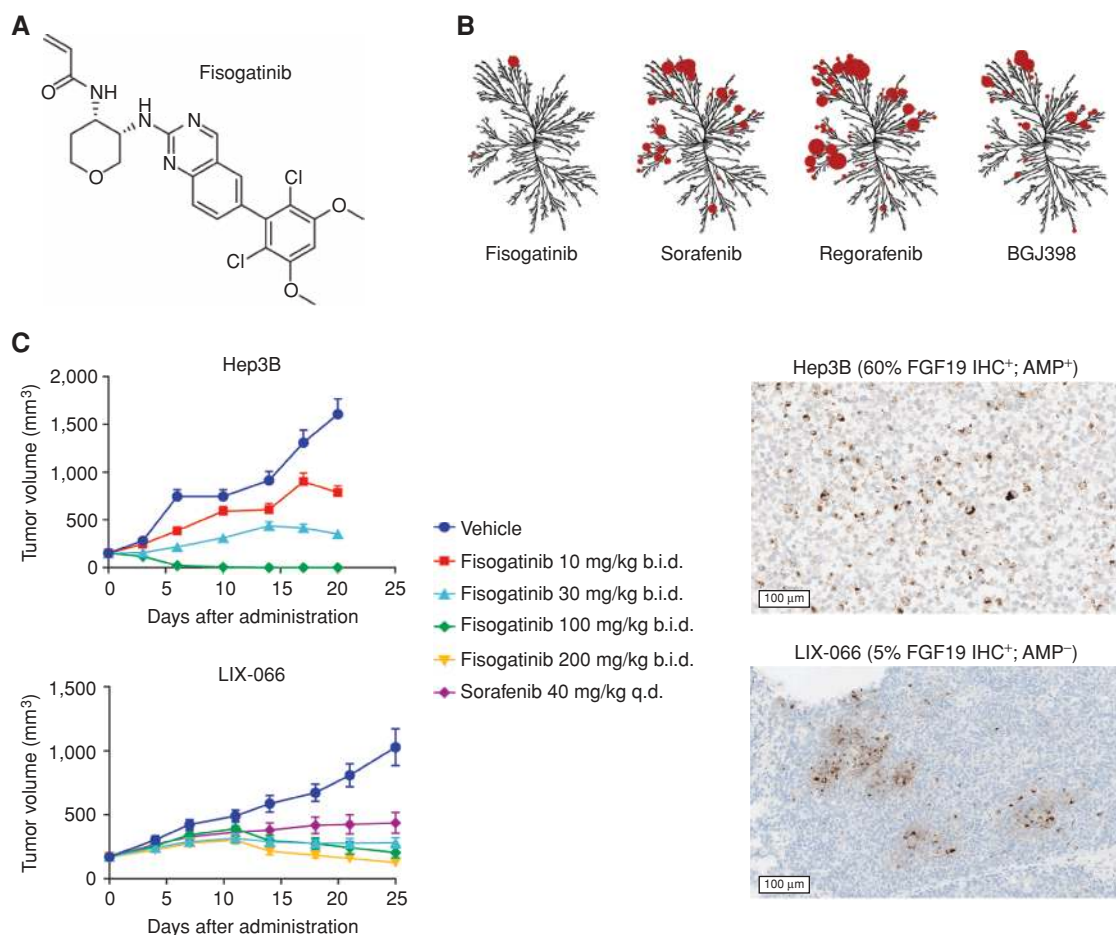


Figure 1. Fisogatinib selectively inhibits FGFR4 and reduces tumor size in preclinical mouse models of FGF19-positive HCC. **A**, Structure of fisogatinib. **B**, Kinome trees depicting the potency (radius) with which fisogatinib, sorafenib, and BGJ398 bind to kinases. **C**, *In vivo* antitumor efficacy of fisogatinib in mice with Hep3B or LIX-066 xenograft tumors. Both models are FGF19-positive by IHC.

risk of recurrence in patients with HCC and was correlated with poor prognostic factors such as high α -fetoprotein and microvascular invasion (21).

We developed fisogatinib (BLU-554), a potent and highly selective oral FGFR4 inhibitor optimized for clinical use, and an accompanying IHC assay to detect aberrant FGF19 expression for use as a potential marker of pathway activation. A phase I first-in-human trial in patients with advanced HCC was conducted to assess the safety, pharmacokinetics (PK), pharmacodynamics (PD), and preliminary clinical activity of fisogatinib and to define the clinical utility of FGF19 IHC as a predictive marker of response.

RESULTS

Fisogatinib Selectively Inhibits FGFR4

Fisogatinib was designed to be a potent, highly selective, small-molecule inhibitor of FGFR4 (Fig. 1A). Fisogatinib covalently binds a unique cysteine residue found in FGFR4 (Cys 552; Supplementary Fig. S1A), thereby conferring a very high degree of selectivity for FGFR4 over other FGFR family members (22) and across the kinome (Fig. 1B). This

selectivity and potent inhibition of FGFR4 were particularly notable when compared with sorafenib, regorafenib, and the pan-FGFR inhibitor BGJ398, which inhibit a broader range of targets across the kinome (Fig. 1B). Fisogatinib also has a high affinity for FGFR4 that is approximately 100-fold higher than its affinity for FGFR1 and almost 1,000-fold higher than its affinity for FGFR2 and FGFR3 (22). Fisogatinib dose-dependently blocked the downstream signaling of FGFR4 in Hep3B cells that were further activated with exogenous FGF19 and in MDA-MB-453 cells with mutated and constitutively active FGFR4 (Supplementary Fig. S1B and S1C; ref. 23). Conversely, fisogatinib did not affect the downstream components of FGFR1 in the lung carcinoma cell line DMS114 when stimulated with FGF2, further confirming the selectivity of this compound (Supplementary Fig. S1D).

To assess the potential utility of FGF19 IHC expression as a marker of pathway activation, we examined the activity of fisogatinib in FGF19 IHC-positive and IHC-negative HCC xenografts. Fisogatinib induced potent, dose-dependent tumor regressions in FGF19 IHC-positive xenografts (Fig. 1C). By contrast, FGF19-negative tumor lines were

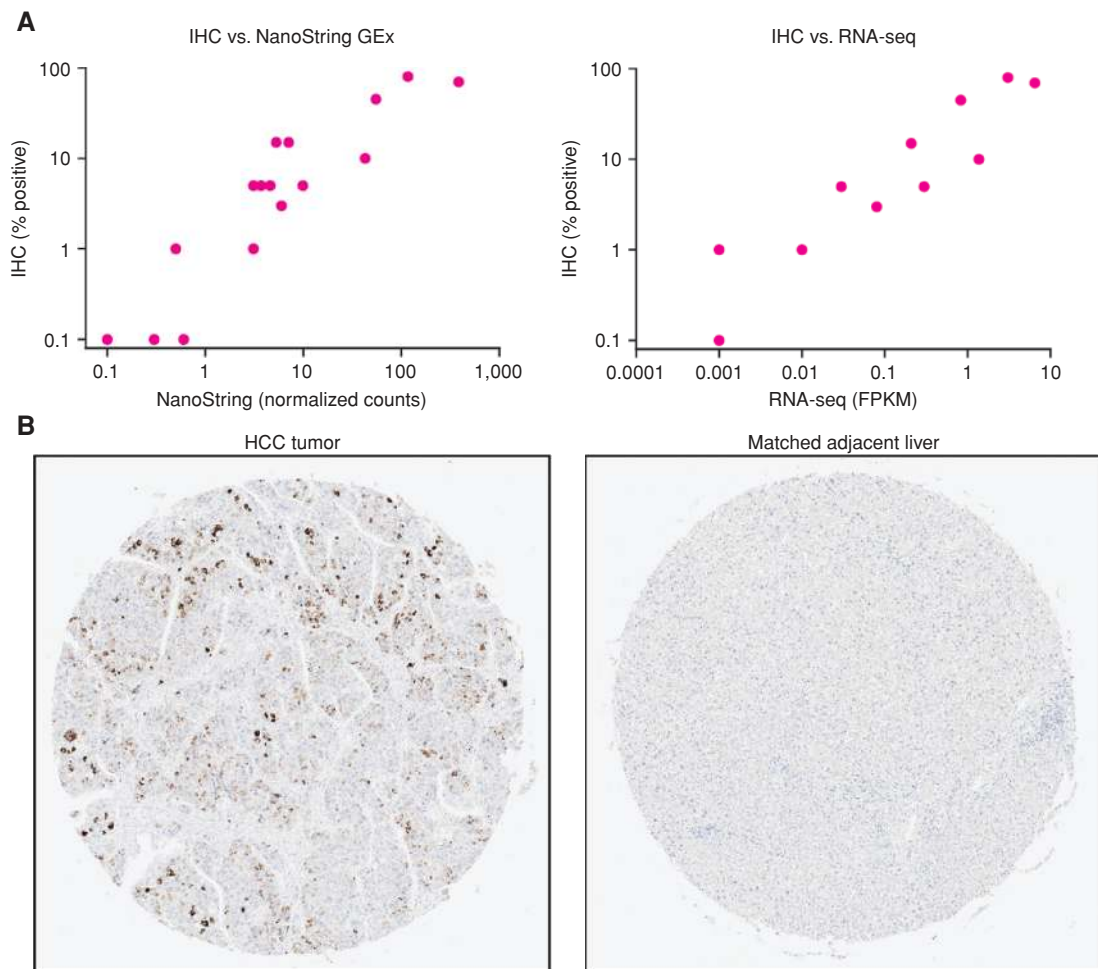


Figure 2. FGF19 positivity by IHC. **A**, FGF19 protein levels measured by IHC show a high concordance with *FGF19* mRNA levels measured with NanoString (left) and RNA-seq (right). **B**, FGF19 measured by IHC in a tumor with positive FGF19 expression (left) and adjacent normal liver tissue (right). GEx, gene expression.

resistant to fisolgatinib treatment (Supplementary Fig. S2A and S2B). Fisolgatinib activity was independent of the level of IHC positivity and was comparable in models with (Hep3B) and without (*LIX-066*) *FGF19* genomic amplification. Tumor regressions were more pronounced with fisolgatinib than with sorafenib (Fig. 1C).

FGF19 IHC as a Biomarker for Patient Selection

Because there is consistent expression of FGFR4 and KLB in normal liver and HCC samples (Supplementary Fig. S3A and S3B), we focused our diagnostic efforts on the variable expression of *FGF19* in HCC. IHC was selected because it requires limited amounts of tissue, is available worldwide, and has the capacity to generate reliable and reproducible results with quick assay turnaround times. A central laboratory assay was developed for clinical trial use, and staining of $\geq 1\%$ of cells was chosen as an initial positivity cutoff based on concordance with *FGF19* mRNA expression (Fig. 2A). Using this assay, we demonstrated *FGF19* expression in a subset of HCC tissues but not in adjacent normal liver (Fig. 2B). Of 395 samples tested, 27% were positive for *FGF19* staining $\geq 1\%$

above baseline. *FGF19* positivity by IHC was well correlated with *FGF19* mRNA levels (Fig. 2A).

Patient Population and Disposition

This first-in-human study used a 3 + 3 dose escalation followed by a maximum tolerated dose (MTD) dose-expansion design (Supplementary Fig. S4A). Additional patients could be enrolled to receive dose levels that were declared tolerable. Once-daily (q.d.) and twice-daily (b.i.d.) schedules were explored. For dose escalations, *FGF19* tumor expression was assessed retrospectively. For dose expansion, *FGF19* tumor expression was assessed prospectively to enroll *FGF19* IHC-positive and *FGF19* IHC-negative cohorts. A total of 115 patients were enrolled in the study (Supplementary Table S1). Most patients (90%) were on their second or later line of therapy; the median number of prior therapies in the total population was 1 (range, 0–5). On the q.d. schedule, 106 patients (25 patients in dose escalation; 81 patients in dose expansion), most of whom had been previously treated with sorafenib (85%), were enrolled (Supplementary Fig. S4A). In the q.d. dose-escalation phase, patients were treated with

140 mg ($n = 3$), 280 mg ($n = 3$), 420 mg, ($n = 6$), 600 mg ($n = 6$), or 900 mg ($n = 7$); the starting dose was 140 mg. After completion of the q.d. dose escalation, a b.i.d. schedule was explored; the starting dose was 200 mg b.i.d. (400 mg total daily dose, $n = 6$), which was escalated to 300 mg b.i.d. (600 mg total daily dose, $n = 3$).

Of all 115 patients enrolled in the study, 63% were positive for FGF19 by IHC. A subset of 53 patients with FGF19-positive tumors by IHC who had available tissue were assessed for *FGFR4* and *KLB* mRNA expression. Importantly, essentially all ($n = 51$, 96%) FGF19-positive patients in this study also showed *FGFR4* and *KLB* expression by RNA sequencing (RNA-seq; Supplementary Fig. S4B), confirming *FGFR4* pathway integrity. Most patients had metastatic disease and had previously been treated with surgery, transarterial chemoembolization, and systemic therapy, such as sorafenib or other multikinase inhibitors (Table 1). Infections from hepatitis B virus or hepatitis C virus were the most common HCC etiologies. Patients with FGF19 IHC-positive tumors were more likely to have α -fetoprotein levels ≥ 400 ng/mL ($P = 0.002$) and trended toward being more likely to have macrovascular invasion ($P = 0.13$) than patients with FGF19 IHC-negative tumors, indicating that FGF19 positivity was correlated with poor prognostic factors, in line with a previous study (21).

Patients in the q.d. cohorts remained on treatment for a median of 2.1 months (range, 0.2–15.2 months), and patients in the b.i.d. cohorts remained on treatment for a median of 2.1 months (range, 0.2–19.6 months). At the time of the data cutoff, 5 patients (5%) continued treatment on the q.d. dosing schedule and none continued treatment on the b.i.d. dosing schedule. The most common reasons for discontinuing treatment in the total population were progressive disease (75%) and adverse events (AE; 13%; Supplementary Table S2).

Safety

In the q.d. dose-escalation phase, no dose-limiting toxicities (DLT) were observed in patients after 1 cycle of fisolatinib with doses of 140 to 600 mg. In the 900-mg cohort, 2 DLTs (1 case of grade 3 abdominal pain and 1 case of grade 3 fatigue lasting > 7 days) were observed (Supplementary Table S3). Therefore, 600 mg was considered the MTD and was selected for the dose-expansion phase.

In the b.i.d. dose escalation, no DLTs were observed in the initial 3 patients enrolled in the 200-mg b.i.d. cohort. Subsequently, 1 DLT of grade 3 pulmonary edema was observed in 3 patients treated with 300-mg b.i.d. fisolatinib. Of 3 additional patients who received 200-mg b.i.d. fisolatinib, 2 DLTs of clinically intolerable grade 2 nausea, vomiting, and diarrhea were observed, indicating that the MTD had been exceeded at these dose levels. Because of less-favorable tolerability observed with b.i.d. dosing (Supplementary Tables S4 and S5) and lower overall dose intensity relative to the q.d. schedule, a b.i.d. dose expansion was not pursued.

Across all dose levels in the q.d. dose-escalation and dose-expansion cohorts, 13 patients (12%) experienced AEs leading to discontinuation of fisolatinib, with 8 of 13 discontinuations being from AEs considered related to fiso-

gatinib. These AEs included fatigue ($n = 4$), abdominal pain, increased alanine aminotransferase, increased aspartate aminotransferase, increased blood bilirubin, diarrhea, and pyrexia ($n = 1$ each). The majority (53%) of treatment-related AEs in the q.d. cohorts were grade 1 or 2. The most common treatment-related AEs in patients treated with q.d. fisolatinib were diarrhea (74%), nausea (42%), and vomiting (35%), which are expected on-target toxicities related to enhanced bile-acid secretion (Table 2). These AEs were manageable with supportive care and dose interruption or reduction. Grade ≥ 3 treatment-related AEs occurred in 46 patients overall (43%), with the most common being elevated aspartate aminotransferase (16/106, 15%) and alanine aminotransferase (12/106, 11%) levels. Grade ≥ 3 diarrhea, vomiting, and nausea occurred in 8 (8%), 4 (4%), and 2 (2%) patients, respectively. Serious AEs of any grade occurred in 46 patients (43%) in the q.d. dosing cohorts, with the most common being disease progression ($n = 5$), hepatic failure ($n = 4$), anemia ($n = 3$), elevated blood bilirubin ($n = 3$), pyrexia ($n = 3$), and vomiting ($n = 3$). There were no treatment-related deaths in the b.i.d. or q.d. dosing groups. Treatment-emergent grade 5 AEs were experienced by 10 patients in the q.d. dosing cohorts, and none were related to fisolatinib (Supplementary Table S6). Additional treatment-emergent AEs for the q.d. dosing cohorts are listed in Supplementary Table S6.

Pharmacokinetics and Pharmacodynamics in the Dose-Escalation Phase

To assess fisolatinib exposure in patients, blood was collected before dosing with fisolatinib and at prespecified time points following dosing on cycle 1, day 1 (C1D1) and on cycle 1, day 15 (C1D15). Following administration of single oral doses of fisolatinib ranging from 140 to 900 mg q.d., the median time to peak concentration (T_{max}) ranged from 1.5 to 2 hours after dosing (Fig. 3A). The mean plasma elimination half-life ($t_{1/2}$) of fisolatinib was 16.5 hours. Systemic exposure to fisolatinib increased in a dose-dependent manner after a single dose on C1D1 and repeat dosing on C1D15. There was no significant drug accumulation [accumulation ratio (Rac) ≤ 1.5] after repeat dosing of fisolatinib, consistent with the observed half-life. At C1D15, the steady-state geometric mean (%CV; n) for the maximum plasma concentration (C_{max}) and area under the curve (AUC) of fisolatinib at the 600-mg q.d. dose was 8,925 ng/mL (33.5%; $n = 70$) and 91,742 h \times ng/mL (42%; $n = 64$), respectively. This exposure to fisolatinib was within the expected therapeutic range based on nonclinical data in xenograft models, supporting 600 mg q.d. as the recommended phase II dose.

FGFR4 pathway activation by FGF19 promotes bile-acid production from cholesterol (24). To study the effects of fisolatinib on *FGFR4* pathway activity, fasting blood samples were collected from patients and assessed for plasma or serum cholesterol, bile-acid precursors, and FGF19. As would be expected from *FGFR4* pathway inhibition, levels of plasma cholesterol were reduced in a dose-dependent manner after treatment, whereas levels of bile acid increased after treatment, reflecting derepression of bile-acid synthesis. In addition, levels of serum FGF19 increased in a dose-dependent manner due to release of negative feedback (Fig. 3B–D).

Table 2. TRAEs in ≥10% of all patients treated with once-daily dosing

TRAE	140 mg (n = 3)		280 mg (n = 3)		420 mg (n = 6)		600 mg (n = 87)		900 mg (n = 7)		All patients (q.d.) (n = 106)	
	Any grade	Grade ≥3	Any grade	Grade ≥3	Any grade	Grade ≥3	Any grade	Grade ≥3	Any grade	Grade ≥3	Any grade	Grade ≥3
Any TRAE	3 (100)	1 (33)	3 (100)	1 (33)	6 (100)	5 (83)	83 (95)	36 (41)	7 (100)	3 (43)	102 (96)	46 (43)
Diarrhea	1 (33)	0 (0)	3 (100)	0 (0)	5 (83)	2 (33)	63 (72)	6 (7)	6 (86)	0 (0)	78 (74)	8 (8)
Nausea	0 (0)	0 (0)	1 (33)	0 (0)	3 (50)	0 (0)	34 (39)	2 (2)	6 (86)	0 (0)	44 (42)	2 (2)
Vomiting	0 (0)	0 (0)	1 (33)	0 (0)	2 (33)	0 (0)	29 (33)	4 (5)	5 (71)	0 (0)	37 (35)	4 (4)
ALT increased	0 (0)	0 (0)	1 (33)	0 (0)	4 (67)	2 (33)	27 (31)	10 (11)	0 (0)	0 (0)	32 (30)	12 (11)
AST increased	0 (0)	0 (0)	1 (33)	1 (33)	4 (67)	2 (33)	24 (28)	13 (15)	0 (0)	0 (0)	29 (27)	16 (15)
Fatigue	1 (33)	0 (0)	1 (33)	0 (0)	0 (0)	0 (0)	19 (22)	3 (3)	4 (57)	1 (14)	25 (24)	4 (4)
Blood bilirubin increased	0 (0)	0 (0)	1 (33)	0 (0)	4 (67)	1 (17)	14 (16)	3 (3)	0 (0)	0 (0)	19 (18)	4 (4)
Decreased appetite	0 (0)	0 (0)	0 (0)	0 (0)	0 (0)	0 (0)	14 (16)	0 (0)	4 (57)	0 (0)	18 (17)	0 (0)
Abdominal pain	1 (33)	0 (0)	1 (33)	0 (0)	1 (17)	0 (0)	7 (8)	0 (0)	4 (57)	1 (14)	14 (13)	1 (1)
Blood ALP increased	0 (0)	0 (0)	1 (33)	0 (0)	3 (50)	1 (17)	9 (10)	3 (3)	0 (0)	0 (0)	13 (12)	4 (4)
Anemia	1 (33)	1 (33)	1 (33)	1 (33)	1 (17)	1 (17)	8 (9)	2 (2)	0 (0)	0 (0)	11 (10)	5 (5)

Abbreviations: ALP, alkaline phosphatase; ALT, alanine aminotransferase; AST, aspartate aminotransferase; q.d., once daily; TRAE, treatment-related adverse event.

Clinical Activity

Across 106 patients treated with q.d. dosing, 98 were evaluable for response assessments per RECIST v1.1 with measurable disease at baseline and at least 1 post-baseline radiographic response assessment. Sixty-six patients with FGF19-positive tumors were evaluable for response, and the overall response rate (ORR) in this population was 17% (11 of 66 patients), with 1 complete response (CR; 2%) and 10 partial responses (PR; 15%; Fig. 4A; Table 3). Three patients remained in response at the time of data cutoff. One patient experienced a PR in the 280-mg cohort, 2 in the 420-mg cohort, and 7 in the 600-mg cohort; the patient who experienced a CR was in the 600-mg cohort. Responses were observed across a wide range of FGF19 IHC positivity (Supplementary Table S7). Eight of the 11 responders had received prior sorafenib. Radiographic tumor reduction and response per RECIST v1.1 were observed in 41% of patients with (*FGF19* FISH-positive) and without (*FGF19* FISH-negative) *FGF19* genomic amplification. Response typically occurred at the first radiographic assessment (2 months); the median duration of response (DOR) for responding patients with FGF19-positive tumors was 5.3 months (95% CI, 3.7 months–not reached; Fig. 4B; Table 3), and the median PFS was 3.3 months (95% CI, 2.1–3.7 months). Eight of the responding patients had responses > 6 months (Fig. 4C).

Of the 34 patients who had FGF19-negative tumors or an unknown FGF19 status ($n = 29$ FGF19 negative; $n = 5$ unknown), 32 were evaluable for response assessments. Per RECIST v1.1, the ORR in these patients was 0% (0 of 32

patients), with 16 patients (50%) having stable disease and 16 patients (50%) having progressive disease as a best response (Table 3; Fig. 4D). The median PFS was 2.3 months (95% CI, 1.8–5.5) in patients with FGF19 IHC-negative tumors.

DISCUSSION

Effective treatment options for advanced HCC are limited compared with other tumor types, and there have been few biomarker-driven targeted therapies identified to date (25). Although the FGF19–FGFR4 pathway has been implicated in hepatocarcinogenesis for more than a decade, no approach has demonstrated the oncogenic importance of this pathway in human HCC to date (12, 17, 18). This phase I study with the highly potent and selective FGFR4 inhibitor fsgatinib clinically validates the therapeutic potential of targeting the FGF19–FGFR4 pathway by demonstrating for the first time that FGFR4 inhibition is tolerable and efficacious in advanced HCC expressing FGF19. The findings of this study, together with the identification of on-target fsgatinib-resistance mutations in FGFR4 (22), confirm the driver status of the FGF19–FGFR4 pathway in HCC with FGF19 overexpression.

FGF19 overexpression is present in a notable proportion of patients with HCC; this study identified FGF19 overexpression by IHC in 27% of HCC tumor samples, consistent with previous reports (3, 20). Previous nonclinical studies with monoclonal antibodies targeting the FGF19–FGFR4 pathway suggested low therapeutic index related to

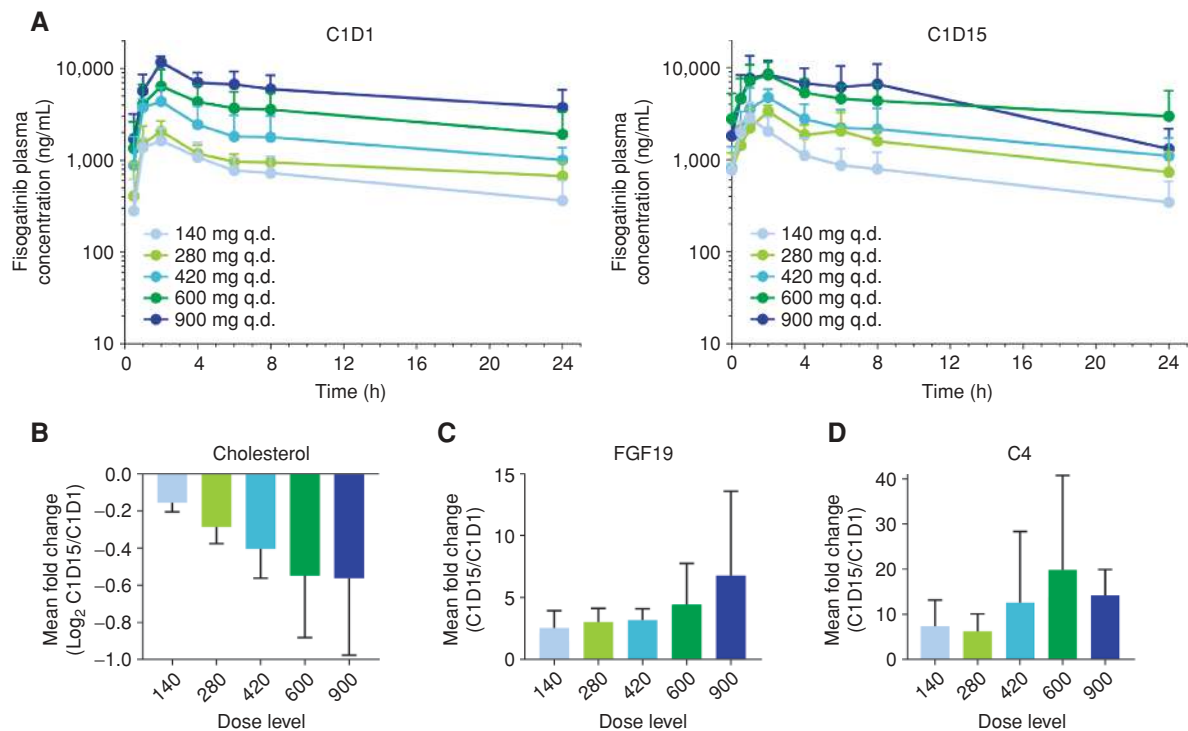


Figure 3. Pharmacokinetics of fisogatinib and pharmacodynamics of blood markers in patients treated with q.d. fisogatinib. **A**, Plasma fisogatinib concentrations over time (cycle 1, day 1). **B–D**, Plasma cholesterol (**B**), bile-acid precursor (C4; **C**), and FGF19 (**D**) levels before and after exposure to fisogatinib. C4, 7 α -hydroxy-4-cholesten-3-one bile acid; C, cycle; D, dose; q.d., once daily.

profound perturbations in bile-acid metabolism (26); therefore, these agents did not advance in clinical testing. Our study demonstrates the feasibility and tolerability of targeting the FGF19–FGFR4 pathway with a small-molecule approach. Notably, fisogatinib was tolerable across multiple dose levels that modulated the FGFR4 pathway and had antitumor activity. As expected, the most common AEs were on-target toxicities related to enhanced bile-acid synthesis, including nausea, vomiting, and diarrhea. At the 600-mg q.d. recommended phase II dose, these events were readily managed with antiemetics and supportive care. The b.i.d. schedule had more prominent on-target toxicity and was less well tolerated, perhaps related to more continuous FGFR4 inhibition. In contrast with pan-FGFR4 inhibitors (20, 27), no hyperphosphatemia was observed with fisogatinib treatment across all dose levels, confirming the exquisite selectivity of fisogatinib for FGFR4. Overall, these data indicate that selective FGFR4 inhibition via a small-molecule approach is feasible and tolerable; however, it is dependent on dose and schedule.

Fisogatinib demonstrated favorable PK properties with rapid absorption, dose-dependent PK with moderate variability, and a half-life of approximately 17 hours, supporting q.d. dosing. Following q.d. dosing, a steady-state level of fisogatinib was reached within 15 days. Accompanying PD data demonstrated that fisogatinib modulates the FGFR4 pathway in a dose-dependent manner, as evidenced by changes in circulating pathway markers (total cholesterol and FGF19). At the recommended phase II dose of 600 mg q.d. fisogatinib, nearly all patients had evidence of FGFR4

pathway modulation, and steady-state exposure was in the expected therapeutic range based on nonclinical studies. Together, these data support further investigation of this dose in future studies.

Targeting FGFR4 with fisogatinib induced radiographic response per RECIST v1.1 in approximately 17% of FGF19 IHC-positive patients and provided radiographic tumor reductions in 41% of FGF19 IHC-positive patients, regardless of their HCC etiology. This is particularly encouraging given that most patients in this study had metastatic disease, poor prognostic disease characteristics, and prior treatment with sorafenib. Previous studies with kinase inhibitors, including regorafenib, cabozantinib, brivanib, and others in the post-sorafenib setting, have shown little or no response per RECIST v1.1 (4, 7, 28). In patients with FGF19-positive tumors, response rates to fisogatinib were similar to those reported for single-agent pembrolizumab and nivolumab in patients with HCC (5, 8). The DOR and clinical benefit rate at 4 months with fisogatinib were also encouraging for the post-sorafenib setting, particularly considering that FGF19 IHC-positive patients were more likely to have poor prognostic factors, including high α -fetoprotein and macrovascular invasion. In contrast with FGF19 IHC-positive patients, FGF19 IHC-negative patients had no response and little disease stabilization. Together, these data indicate that FGF19 IHC positivity increases the likelihood of response with fisogatinib and suggest that IHC positivity may be a surrogate of pathway activation.

Given the marked heterogeneity of HCC, additional translational studies with the FGF19 IHC assay and evaluation of

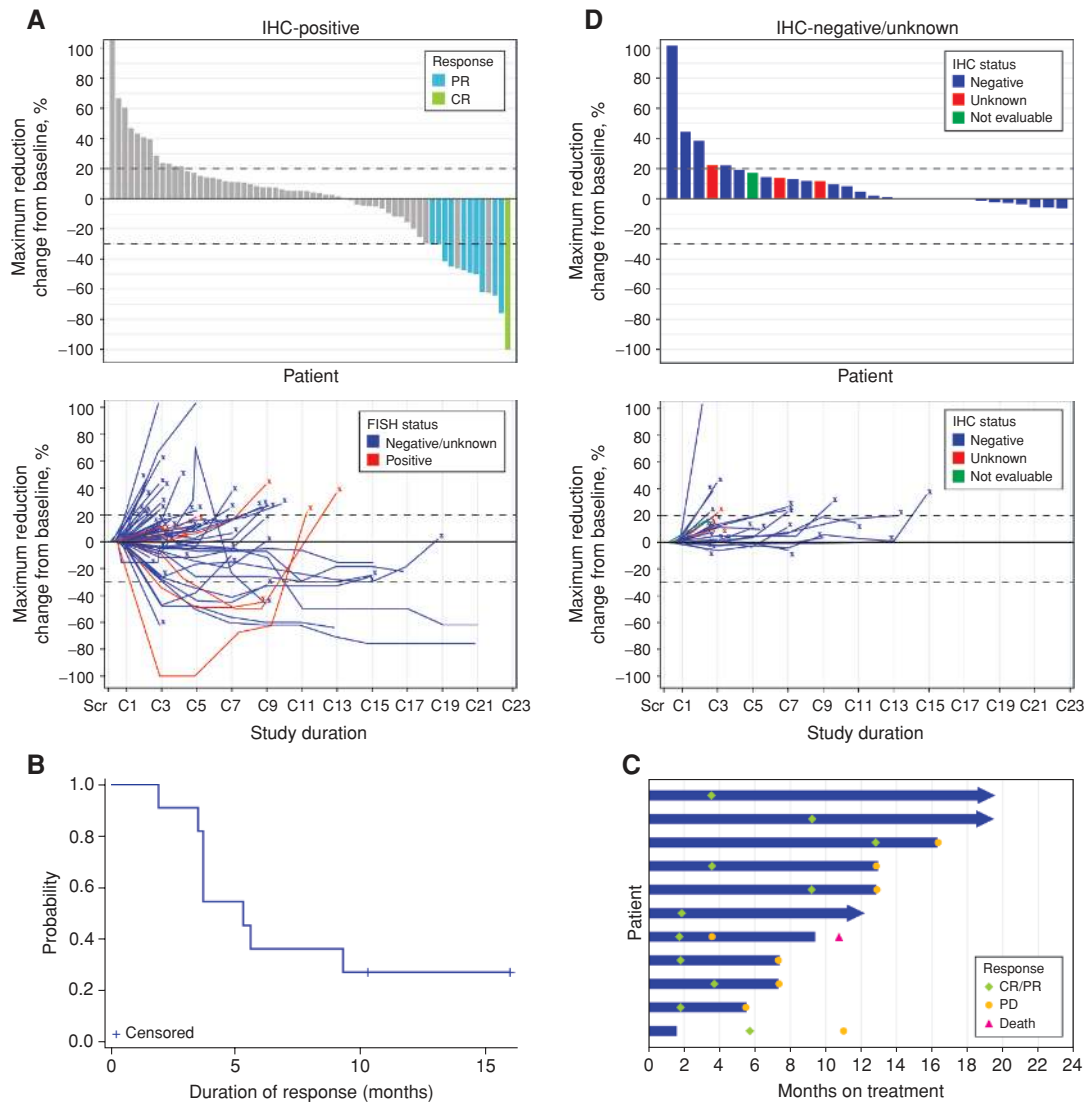


Figure 4. Response to fisogatinib by FGF19 IHC positivity. **A**, Waterfall plot showing the percentage maximum reduction in tumor size from baseline (top) and spider plot showing the maximum reduction in tumor size from baseline over time (bottom) in patients with FGF19-positive tumors. **B**, Kaplan-Meier curve of DOR in responding patients. **C**, Swim lane plot showing patient responses and outcomes over time. **D**, Waterfall plot showing the percentage maximum reduction in tumor size from baseline (top) and spider plot showing the maximum reduction in tumor size from baseline over time (bottom) in patients with FGF19-negative/unknown tumors. CR, complete response; PD, progressive disease; PR, partial response.

other novel biomarkers could further optimize the selection of patients most likely to benefit from fisogatinib treatment. Notably, the level of IHC positivity was not correlated with response or genomic amplification of the *FGF19* locus. This could relate to a limited dynamic range of the assay or heterogeneity of FGF19 expression across different tumor lesions. Alternatively, any level of FGF19 expression may indicate an oncogenic state driven by a minimal threshold of ligand concentration. Evaluation of tumor *FGF19* RNA expression may offer a more sensitive and dynamic method for evaluating potential responders. Activation of other oncogenic pathways implicated in hepatocarcinogenesis may further modulate the response to fisogatinib (15). Interrogation of these pathways in tumor and circulating tumor DNA is feasible using next-generation sequencing. Additional studies regarding

this are under way, and the results of these investigations may further refine patient selection.

In conclusion, the findings from this study of fisogatinib demonstrate for the first time that FGFR4 inhibition is tolerable and clinically active in advanced HCC expressing FGF19. PK, PD, safety, and antitumor activity data support a continuous q.d. dosing schedule for fisogatinib for further clinical investigation. This study illustrates that FGFR4 signaling is targetable by small molecules for effective, biomarker-driven treatment of HCC. Based on these data and recent data suggesting enhanced efficacy with combinations of targeted therapies and checkpoint inhibitors (29–31), we are pursuing further development of fisogatinib in FGF19-positive patients both as a monotherapy and in combination with immunotherapy.

Table 3. Preliminary clinical activity

Outcome	FGF19-positive (n = 66)	FGF19-negative/unknown ^a (n = 32)
Best response, n (%)		
Overall response rate	11 (17)	0 (0)
Complete response	1 (2)	0 (0)
Partial response	10 (15)	0 (0)
Stable disease	30 (45)	16 (50)
Progressive disease	25 (38)	16 (50)
Median DOR (95% CI), months	5.3 (3.7-NE)	-
Median PFS (95% CI), months	3.3 (2.1-3.7)	2.3 (1.8-5.5)

Abbreviations: DOR, duration of response; NE, not estimable.

^aThree patients had unknown FGF19 status; 1 patient had FGF19 that was not evaluable.

METHODS

Study Design and Patients

This was a phase I, open-label, first-in-human study designed to evaluate the safety, tolerability, PK, PD, and preliminary antineoplastic activity of figogatinib administered orally in patients with HCC. The study started on July 22, 2015, and was conducted at 21 study sites in 10 countries or territories (the United States, South Korea, the United Kingdom, Spain, France, Italy, China, Taiwan, Singapore, Germany, and Switzerland). For dose escalation, FGF19 IHC was assessed retrospectively. For dose expansion, FGF19 IHC was assessed prospectively to enroll ~60 IHC-positive and ~15 IHC-negative patients in expansion cohorts.

Eligible patients were ≥ 18 years of age with a confirmed HCC diagnosis per histology or noninvasive criteria guidelines (European Association for the Study of the Liver or American Association for the Study of Liver Diseases; ref. 32) and unresectable disease; they were treatment-naïve (had declined or did not have access to sorafenib) or previously treated with sorafenib. In the dose-escalation phase, patients provided archived tumor tissue (if available) and had pretreatment and on-treatment tumor biopsy specimens collected if deemed appropriate by the treating physician. In the dose-expansion phase, patients had ≥ 1 target lesion per RECIST v1.1 and available FGF19 by IHC results. *FGF19* by FISH was continually measured to retrospectively stratify patients. Patients were required to have an Eastern Cooperative Oncology Group performance status of 0 or 1 and a Child–Pugh score of 5 or 6 points (class A), with no clinically apparent ascites. Patients with hepatitis C virus infection must have completed curative antiviral therapy, if indicated and available, before receiving the first dose of figogatinib. In patients with hepatitis B virus infection, treatment with antiviral therapy was not required before enrollment and was allowed during the study, unless otherwise contraindicated with figogatinib.

This study was conducted in accordance with the protocol, good clinical practice standards, and the Declaration of Helsinki. The appropriate institutional review board or ethics committee of each participating institution approved the protocol. All enrolled patients provided written informed consent before undergoing study-specific procedures. To identify patients with FGF19-positive tumors, a separate screening Informed Consent Form was available.

Treatments

Synthesis of figogatinib was described in the patent application WO2015/061572A1. The dose-escalation phase of the study used a 3 + 3 design in which cohorts of 3 patients received the following dose levels of oral figogatinib on a q.d. schedule to determine the

MTD and recommended phase II dose: 140, 280, 420, 600, and 900 mg. A second dose-escalation cohort of patients receiving figogatinib was evaluated using a b.i.d. dosing schedule at a starting dose of 200 mg. Each cycle lasted 28 days. DLT was defined as any treatment-emergent AE of grade ≥ 3 occurring during cycle 1 that was not clearly caused by something other than figogatinib. The dose-determining population included all patients in the dose-escalation phase who received $\geq 75\%$ of figogatinib in cycle 1 and completed cycle 1 or experienced a DLT. The dose-expansion phase of the study enrolled patients who were treated with figogatinib at the recommended phase II dose.

Endpoints

The primary objectives were to determine the MTD and recommended phase II dose of figogatinib and to assess safety and tolerability. Secondary objectives included characterization of the PK and PD profiles, definition of FGF19 status in tumor tissue via IHC and FISH, and assessment of preliminary evidence of antitumor activity per RECIST v1.1.

Assessments

Patients without documented disease progression were followed for disease assessment approximately every 3 months until disease progression, the start of another antineoplastic therapy, or death. AEs were assessed for intensity according to the NCI's Common Terminology Criteria for Adverse Events, version 4.03. Treatment-emergent AEs were defined as any AE that occurred during or after administration of the first dose of figogatinib through 30 days after the last dose of figogatinib; any event considered related to study drug, regardless of the start date of the event; or any event that was present at baseline but worsened in intensity or was subsequently considered related to study drug by the investigator.

Figogatinib activity was assessed based on the ORR (defined as the rate of CR + PR) per RECIST v1.1 and the DOR. The response-evaluable population included all patients dosed in the dose-expansion phase who had measurable disease per RECIST v1.1 at baseline and ≥ 1 post-baseline disease response assessment performed on cycle 3 day 1 and received $\geq 75\%$ of figogatinib in cycle 1.

The following PK parameters of figogatinib were assessed as appropriate following single-dose administration and at steady state: C_{max} ; T_{max} ; AUC from 0 to 24 hours; $t_{1/2}$; apparent oral clearance (CL/F); apparent volume of distribution (V_z/F); and Rac. The following PD parameters were assessed: changes in blood including, but not limited to, changes in blood FGF19 (part 1 only); cholesterol; bile-acid precursors [e.g., 7 α -hydroxy-4-cholesten-3-one (cycle 4), part 1 only]; α -fetoprotein; and changes in tumor Ki-67 and cleaved caspase-3 levels.

IHC Assay Development

An assay using an FGF19 rabbit monoclonal antibody (clone SP268, Roche Tissue Diagnostics) was optimized for use as a fully automated IHC assay on the BenchMark ULTRA (Roche Tissue Diagnostics) staining platform using the OptiView DAB IHC Detection Kit and OptiView Amplification Kit (Roche Tissue Diagnostics). The assay was optimized for detection of FGF19 protein expression in formalin-fixed, paraffin-embedded HCC tissue. Parameters evaluated during optimization included antibody concentration, antibody diluent, antigen retrieval method, antibody incubation conditions, and counterstain conditions. In addition, signal amplification using the OptiView Amplification Kit (Roche Tissue Diagnostics) was tested to evaluate its efficacy in visualizing specific signals. The optimal conditions for tumor-cell staining in HCC tissue on the BenchMark ULTRA instrument are outlined in Supplementary Table S8. Briefly, antigen retrieval was undertaken for 16 minutes, the primary antibody was applied for 16 minutes at 36°C, and amplification was conducted for 8 minutes amplifier/8 minutes multimer. Samples were counterstained for 8 minutes with hematoxylin II and post-counterstained for 8 minutes.

Statistical Analyses

Descriptive analyses were used to characterize safety, PK, PD, and efficacy. The Kaplan-Meier method was used to estimate medians for DOR and PFS. The 95% CIs for DOR and PFS were obtained using linear transformation. This study is registered with ClinicalTrials.gov as NCT02508467.

Study Oversight

This study was designed, conducted, and analyzed by Blueprint Medicines in conjunction with the authors. All authors revised and provided input to the manuscript and made the decision to submit for publication. The authors had access to all data and vouch for the validity of the study results reported herein and adherence to the protocol. The study was performed with the ethical principles of the Declaration of Helsinki and was consistent with the International Conference on Harmonization/Good Clinical Practice and applicable regulatory requirements. The institutional review board or independent ethics committee of each study center approved the study.

Disclosure of Potential Conflicts of Interest

R.D. Kim has received honoraria from the speakers bureaus of Lilly and Taiho, and is an unpaid consultant/advisory board member for Bayer, BMS, and Exelixis. D. Sarker is a consultant at Novartis, Ipsen, and Eisai and has received honoraria from the speakers bureaus of MSD, Pfizer, Ipsen, Bayer, and Eisai. T. Macarulla reports receiving commercial research support from Celgene, AstraZeneca, and BeiGene, has received honoraria from the speakers bureaus of Celgene, Raffo, Serviere, Incyte, and Sanofi, and is an unpaid consultant/advisory board member for Celgene, Serviere, Incyte, Amgen, and AstraZeneca. J.-W. Park is an advisor at Roche-Genentech, Bayer, Ono, Eisai, and Midatech and has received honoraria from the speakers bureaus of Bayer, Ono, and Eisai. S.P. Choo has received honoraria from the speakers bureaus of Lilly Oncology and Bristol-Myers Squibb. J. Trojan is an advisor at BMS, Celgene, Eisai, and Ipsen and has received honoraria from the speakers bureaus of BMS, Lilly, Merck Serono, MSD, Ipsen, and Eisai. A.X. Zhu is a consultant at Bayer, Lilly, Eisai, Merck, Sanofi-Aventis, and Roche-Genentech. J.-H. Yoon reports receiving commercial research grants from AstraZeneca, Bayer HealthCare Pharmaceuticals, Daewoong Pharmaceuticals, and Bukwang Pharmaceuticals. S. Sharma is on the advisory board of Barricade Therapeutics, Exelixis, Dracen Pharmaceuticals, Tarveda Therapeutics, Hengrui Therapeutics, Loxo Oncology, and Natera, Inc., reports receiving a commercial research grant from Salarius Pharmaceuticals, reports receiving other commercial research support from Novartis, GSK,

Toray Industries, Celgene, Hengrui Therapeutics, OncoMed, Tesaro, AADI, Merck, Inhibrx Inc., AMAL Therapeutics, Syndax, Millennium, Johnson & Johnson, Gilead Sciences, Plexikon, Onyx, Blueprint Medicines, XuanZhu, and Incyte, has ownership interest (including patents) in Iterion Therapeutics, Salarius Pharmaceuticals, Proterus Therapeutics, ConverGene, and LSK BioPharma, and is an unpaid consultant/advisory board member for Novartis, Arrien Pharmaceuticals, and Array BioPharma. S. Faivre has received honoraria from the speakers bureaus of Blueprint Medicines, Bristol-Myers Squibb, Bayer, Eli Lilly, Ipsen, Merck Serono, MSD, and Novartis. D.H. Palmer is a speaker and advisor for Bayer, Eisai, BMS, and AstraZeneca, and reports receiving commercial research grants from BMS, AstraZeneca, Sirtex, and BTG. J.M. Llovet is a consultant for Eli Lilly, Bayer Healthcare Pharmaceuticals, Navigant, Leerink Swann LLC, Midatech Ltd., Fortress Biotech Inc., Springbank Pharmaceuticals, Nucleix, Can-Fite, Bristol-Myers Squibb, Eisai Inc., Celsion Corporation, Exelixis, Merck, Blueprint, Ipsen, and Glycotest, and reports receiving commercial research grants from Bayer Healthcare Pharmaceuticals, Eisai Inc., Bristol-Myers Squibb, Boehringer Ingelheim, and Ipsen. M. Manoogian is a scientist at Roche Tissue Diagnostics. M. Tugnait is Senior Director, Clinical Pharmacology, at Blueprint Medicines and has stock options with Blueprint Medicines. N. Stransky is Senior Director at Celsion Therapeutics, and has ownership interest (including patents) in Blueprint Medicines and Celsion Therapeutics. M. Hagel has ownership interest (including patents) in ISO. C. Lengauer is Executive Vice President at Blueprint Medicines, is a partner at Third Rock Ventures, is a director at Hookipa, is a scientific advisory board member for Mersana, and has ownership interest (including patents) in Blueprint Medicines, Third Rock Ventures, Hookipa, and Mersana. C.A. Sherwin is a senior clinical program manager at Blueprint Medicines Corporation. O. Schmidt-Kittler is a principal investigator at Blueprint Medicines and has an ownership interest (including patents) in the same. K.P. Hoeflich is Vice President, Biology, at Blueprint Medicines and has ownership interest (including patents) in the same. H. Shi is Senior Director, Biostatistics and Data Management, at Blueprint Medicines Inc. B.B. Wolf is Senior Vice President, Clinical Development, at Blueprint Medicines and has ownership interest (including patents) in the same. Y.-K. Kang is an unpaid consultant/advisory board member for Blueprint and BMS. No potential conflicts of interest were disclosed by the other authors.

Authors' Contributions

Conception and design: R.D. Kim, T. Yau, A.X. Zhu, J.M. Llovet, C. Lengauer, K.P. Hoeflich, H. Shi, B.B. Wolf, Y.-K. Kang

Development of methodology: R.D. Kim, T. Yau, M. Manoogian, K.P. Hoeflich, H. Shi, B.B. Wolf

Acquisition of data (provided animals, acquired and managed patients, provided facilities, etc.): R.D. Kim, D. Sarker, T. Meyer, T. Yau, T. Macarulla, J.-W. Park, S.P. Choo, A. Hollebecque, M.W. Sung, H.-Y. Lim, V. Mazzaferro, J. Trojan, A.X. Zhu, J.-H. Yoon, S. Sharma, Z.-Z. Lin, S.L. Chan, S. Faivre, L.G. Feun, C.-J. Yen, J.-F. Dufour, D.H. Palmer, C.A. Sherwin, B.B. Wolf, Y.-K. Kang

Analysis and interpretation of data (e.g., statistical analysis, biostatistics, computational analysis): R.D. Kim, D. Sarker, T. Meyer, T. Yau, T. Macarulla, S.P. Choo, H.-Y. Lim, J. Trojan, A.X. Zhu, S. Sharma, S. Faivre, D.H. Palmer, J.M. Llovet, M. Tugnait, N. Stransky, O. Schmidt-Kittler, K.P. Hoeflich, H. Shi, B.B. Wolf, Y.-K. Kang

Writing, review, and/or revision of the manuscript: R.D. Kim, D. Sarker, T. Meyer, T. Yau, T. Macarulla, J.-W. Park, S.P. Choo, A. Hollebecque, M.W. Sung, H.-Y. Lim, V. Mazzaferro, J. Trojan, A.X. Zhu, S. Sharma, S.L. Chan, S. Faivre, C.-J. Yen, J.-F. Dufour, D.H. Palmer, J.M. Llovet, M. Tugnait, C. Lengauer, C.A. Sherwin, O. Schmidt-Kittler, K.P. Hoeflich, H. Shi, B.B. Wolf, Y.-K. Kang

Administrative, technical, or material support (i.e., reporting or organizing data, constructing databases): R.D. Kim, T. Yau, T. Macarulla, H.-Y. Lim, H. Shi

Study supervision: R.D. Kim, D. Sarker, T. Macarulla, M.W. Sung, H.-Y. Lim, A.X. Zhu, J.-H. Yoon, N.E. Kohl, C. Lengauer, K.P. Hoeflich, B.B. Wolf, Y.-K. Kang

Other (discovered compound): M. Hagel

Acknowledgments

The authors thank Maryann Obiorah, PhD, and Allison Cherry, PhD, for medical writing support sponsored by Blueprint Medicines. Kinome illustrations were reproduced courtesy of CSTI (www.cellsignal.com). The foregoing website is maintained by CSTI, and Blueprint Medicines is not responsible for its content. T. Meyer acknowledges support from the UCL Experimental Cancer Medicine Centre and the NIHR UCLH Clinical Research Facility and Biomedical Research Centre. This study was funded by Blueprint Medicines.

Received June 5, 2019; revised August 26, 2019; accepted September 26, 2019; published first October 1, 2019.

REFERENCES

- Llovet JM, Zucman-Rossi J, Pikarsky E, Sangro B, Schwartz M, Sherman M, et al. Hepatocellular carcinoma. *Nat Rev Dis Primers* 2016;2:16018.
- Bray F, Ferlay J, Soerjomataram I, Siegel RL, Torre LA, Jemal A. Global cancer statistics 2018: GLOBOCAN estimates of incidence and mortality worldwide for 36 cancers in 185 countries. *CA Cancer J Clin* 2018; 68:394–424.
- Llovet JM, Montal R, Sia D, Finn RS. Molecular therapies and precision medicine for hepatocellular carcinoma. *Nat Rev Clin Oncol* 2018;15:599–616.
- Abou-Alfa GK, Meyer T, Cheng AL, El-Khoueiry AB, Rimassa L, Ryoo BY, et al. Cabozantinib in patients with advanced and progressing hepatocellular carcinoma. *N Engl J Med* 2018;379:54–63.
- Zhu AX, Finn RS, Edeline J, Cattani S, Ogasawara S, Palmer D, et al. Pembrolizumab in patients with advanced hepatocellular carcinoma previously treated with sorafenib (KEYNOTE-224): a non-randomised, open-label phase 2 trial. *Lancet Oncol* 2018;19:940–52.
- Zhu AX, Kang YK, Yen CJ, Finn RS, Galle PR, Llovet JM, et al. Ramucirumab after sorafenib in patients with advanced hepatocellular carcinoma and increased alpha-fetoprotein concentrations (REACH-2): a randomised, double-blind, placebo-controlled, phase 3 trial. *Lancet Oncol* 2019;20:282–96.
- Bruix J, Qin S, Merle P, Granito A, Huang YH, Bodoky G, et al. Regorafenib for patients with hepatocellular carcinoma who progressed on sorafenib treatment (RESORCE): a randomised, double-blind, placebo-controlled, phase 3 trial. *Lancet* 2017;389:56–66.
- El-Khoueiry AB, Sangro B, Yau T, Crocenzi TS, Kudo M, Hsu C, et al. Nivolumab in patients with advanced hepatocellular carcinoma (CheckMate 040): an open-label, non-comparative, phase 1/2 dose escalation and expansion trial. *Lancet* 2017;389:2492–502.
- Kudo M, Finn RS, Qin S, Han KH, Ikeda K, Piscaglia F, et al. Lenvatinib versus sorafenib in first-line treatment of patients with unresectable hepatocellular carcinoma: a randomised phase 3 non-inferiority trial. *Lancet* 2018;391:1163–73.
- Llovet JM, Ricci S, Mazzaferro V, Hilgard P, Gane E, Blanc JF, et al. Sorafenib in advanced hepatocellular carcinoma. *N Engl J Med* 2008;359:378–90.
- Inagaki T, Choi M, Moschetta A, Peng L, Cummins CL, McDonald JG, et al. Fibroblast growth factor 15 functions as an enterohepatic signal to regulate bile acid homeostasis. *Cell Metab* 2005;2:217–25.
- Sawey ET, Chanrion M, Cai C, Wu G, Zhang J, Zender L, et al. Identification of a therapeutic strategy targeting amplified FGF19 in liver cancer by Oncogenomic screening. *Cancer Cell* 2011;19:347–58.
- Wang K, Lim HY, Shi S, Lee J, Deng S, Xie T, et al. Genomic landscape of copy number aberrations enables the identification of oncogenic drivers in hepatocellular carcinoma. *Hepatology* 2013;58:706–17.
- Schulze K, Imbeaud S, Letouze E, Alexandrov LB, Calderaro J, Rebouissou S, et al. Exome sequencing of hepatocellular carcinomas identifies new mutational signatures and potential therapeutic targets. *Nat Genet* 2015;47:505–11.
- Totoki Y, Tatsuno K, Covington KR, Ueda H, Creighton CJ, Kato M, et al. Trans-ancestry mutational landscape of hepatocellular carcinoma genomes. *Nat Genet* 2014;46:1267–73.
- Hoeflich K, Moeini A, Hagel M, Miduturu C, Sia D, Pinyol R. FGF19 aberrations and selective targeting with FGFR4 inhibitors for hepatocellular carcinoma. In: Proceedings from the International Liver Cancer Association 9th Annual Conference; September 3–6, 2015; Paris, France. Abstract 0-030.
- Nicholes K, Guillet S, Tomlinson E, Hillan K, Wright B, Frantz GD, et al. A mouse model of hepatocellular carcinoma: ectopic expression of fibroblast growth factor 19 in skeletal muscle of transgenic mice. *Am J Pathol* 2002;160:2295–307.
- Wu X, Ge H, Lemon B, Vonderfecht S, Weiszmann J, Hecht R, et al. FGF19-induced hepatocyte proliferation is mediated through FGFR4 activation. *J Biol Chem* 2010;285:5165–70.
- Desnoyers LR, Pai R, Ferrando RE, Hotzel K, Le T, Ross J, et al. Targeting FGF19 inhibits tumor growth in colon cancer xenograft and FGF19 transgenic hepatocellular carcinoma models. *Oncogene* 2008;27:85–97.
- Hagel M, Miduturu C, Sheets M, Rubin N, Weng W, Stransky N, et al. First selective small molecule inhibitor of FGFR4 for the treatment of hepatocellular carcinomas with an activated FGFR4 signaling pathway. *Cancer Discov* 2015;5:424–37.
- Kang HJ, Haq F, Sung CO, Choi J, Hong SM, Eo SH, et al. Characterization of hepatocellular carcinoma patients with FGF19 amplification assessed by fluorescence in situ hybridization: a large cohort study. *Liver Cancer* 2019;8:12–23.
- Hadlen MA, Schmidt-Kittler O, Sherwin CA, Rozahegyi E, Rubin N, Sheets MP, et al. Acquired on-target clinical resistance validates FGFR4 as a driver of hepatocellular carcinoma. *Cancer Discov* 2019;9:1686–95.
- Roidl A, Foo P, Wong W, Mann C, Bechtold S, Berger HJ, et al. The FGFR4 Y367C mutant is a dominant oncogene in MDA-MB453 breast cancer cells. *Oncogene* 2010;29:1543–52.
- DeGirolamo C, Sabba C, Moschetta A. Therapeutic potential of the endocrine fibroblast growth factors FGF19, FGF21 and FGF23. *Nat Rev Drug Discov* 2016;15:51–69.
- Rinninella E, Cerrito L, Spinelli I, Cintoni M, Mele MC, Pompili M, et al. Chemotherapy for hepatocellular carcinoma: current evidence and future perspectives. *J Clin Transl Hepatol* 2017;5:235–48.
- Pai R, French D, Ma N, Hotzel K, Plise E, Salphati L, et al. Antibody-mediated inhibition of fibroblast growth factor 19 results in increased bile acids synthesis and ileal malabsorption of bile acids in cynomolgus monkeys. *Toxicol Sci* 2012;126:446–56.
- Dieci MV, Arnedos M, Andre F, Soria JC. Fibroblast growth factor receptor inhibitors as a cancer treatment: from a biologic rationale to medical perspectives. *Cancer Discov* 2013;3:264–79.
- Johnson PJ, Qin S, Park JW, Poon RT, Raoul JL, Philip PA, et al. Brivanib versus sorafenib as first-line therapy in patients with unresectable, advanced hepatocellular carcinoma: results from the randomized phase III BRISK-FL study. *J Clin Oncol* 2013;31:3517–24.
- Ikeda M, Sung MW, Kudo M, Kobayashi M, Baron AD, Finn RS, et al. A phase 1b trial of lenvatinib (LEN) plus pembrolizumab (PEM) in patients (pts) with unresectable hepatocellular carcinoma (uHCC). *J Clin Oncol* 2018;36(15_suppl):4076.
- Kudo M. Combination cancer immunotherapy in hepatocellular carcinoma. *Liver Cancer* 2018;7:20–7.
- Stein S, Pishvaian MJ, Lee MS, Lee K-H, Hernandez S, Kwan A, et al. Safety and clinical activity of 1L atezolizumab + bevacizumab in a phase Ib study in hepatocellular carcinoma (HCC). *J Clin Oncol* 2018;36(15_suppl):4074.
- Bruix J, Sherman M, Practice Guidelines Committee AaFtSoLD. Management of hepatocellular carcinoma. *Hepatology* 2005;42:1208–36.